LETTERS IN BIOMATHEMATICS
An International Journal

Intercollegiate Biomathematics Alliance

RESEARCH ARTICLE

OPEN ACCESS

Unidirectional Migration of Populations with Allee Effect

Gergely Röst[a], AmirHosein Sadeghimanesh[a,b]

[a]National Laboratory for Health Security, Bolyai Institute, University of Szeged, Aradi vértanúk tere 1, Szeged, H-6720, Hungary; [b]Centre for Computational Sciences and Mathematical Modelling, Coventry University, Innovation Village 10, Cheetah Road, Coventry, CV1 2TL, United Kingdom;

ABSTRACT

In this note we consider two populations living on identical patches, connected by unidirectional migration, and subject to strong Allee effect. We show that by increasing the migration rate, there are more bifurcation sequences than previous works showed. In particular, the number of steady states can change from 9 (small migration) to 3 (large migration) at a single bifurcation point, or via a sequence of bifurcations with the system having 9, 7, 5, 3 steady states or 9, 7, 9, 3 steady states, depending on the Allee threshold. This is in contrast with the case of bidirectional migration, where the number of steady states always goes through the same bifurcation sequence of 9, 5, 3 steady states as we increase the migration rate, regardless of the value of the Allee threshold. These results have practical implications as well in spatial ecology.

ARTICLE HISTORY
Received May 6, 2022
Accepted December 28, 2022

KEYWORDS
population dynamics, migration, bifurcation, steady states, Allee effect, cylindrical algebraic decomposition

1 Introduction

Allee effect is a key concept in population ecology (see Courchamp et al., 2008) and refers to the situation where a population has smaller growth rate at lower densities. In the case of strong Allee effect, there is a critical value called the Allee threshold, such that the population is declining whenever its density is below this threshold. A general problem of high importance in ecology is to describe the effects of diffusion of species on the dynamics of their populations (see Okubo and Levin, 2001). Hence, the interplay of spatial dispersal and Allee effect is of special interest and was the subject of recent works by Gyllenberg et al. (1999); Keitt et al. (2001); Knipl and Röst (2014, 2016); Vortkamp et al. (2020). The problem has practical importance in conservation ecology, biological control, and environmental management.

The goal of this paper is to provide a finer picture of the possible dynamics of a population living on two connected patches, and subject to Allee effect. Our mathematical starting point is Figure 1(a) in the work by Knipl and Röst (2016), which illustrates how the structure of equilibria change in such a model, defined in continuous time . Generally, steady states collide in saddle-node bifurcations and disappear as we increase the migration rate between the patches, and the situation simplifies. However, it is not the case in a discrete time version, where attractors may appear and disappear in the presence of dispersal, as pointed out by Vortkamp et al. (2020). In this note we show that new steady states can appear even in the continuous time model as the migration rate increases, if we allow only one-way (unidirectional) migration between the patches. Here we completely describe the possible bifurcation sequences in the unidirectional case, which is, somewhat surprisingly, more diverse than the bidirectional case. In particular, our results reveal that Figure 2(a) in the work of Knipl and Röst (2016) is incomplete, and there are other possible routes via bifurcation sequences from 9 steady states (small migration) to 3 steady states (large migration). Our main tools are algebraic, and the computational files can be accessed via (Röst and Sadeghimanesh, 2023).

Finally, we discuss the ecological implications of these results, highlighted by the example of coral reef conservation.

2 Two-Patch Model

We consider a single species population model on two identical patches with strong Allee effect and spatial dispersal, and different possible connectivity of the two patches. There exist three non-isomorphic digraphs with two nodes: two disconnected nodes, a fully connected digraph, and finally a directed graph with a source and a target. These three digraphs are shown in Figure 1. Let $N_i(t)$ denote the population at patch i at time t with carrying capacity normalized to 1, let $b \in (0,1)$ be the Allee threshold,

CONTACT AmirHosein Sadeghimanesh ad6397@coventry.ac.uk

and $a \geq 0$ be the spatial dispersal rate. We drop the emphasis on t, and simply write N_i. We also use the notation $\dot{N}_i$ instead of $\frac{dN_i(t)}{dt}$. Then the population of the patches is modelled by the following system:

$$\begin{aligned} \dot{N}_1 &= N_1(1-N_1)(N_1-b) - \delta_{1,2}aN_1 + \delta_{2,1}aN_2, \\ \dot{N}_2 &= N_2(1-N_2)(N_2-b) + \delta_{1,2}aN_1 - \delta_{2,1}aN_2, \end{aligned} \tag{1}$$

where $\delta_{i,j}$ is 1 if there is a directed edge from patch i to patch j, and 0 otherwise. This is the same as Equation $\mathcal{M}_\alpha$ of Knipl and Röst (2016) where the parameter r and the function $g_i(N_i)$ in their notation are chosen as $r = 2$ and $g_i(N_i) = (1-N_i)(N_i-b)$, and when the connectivity graph is fully connected is the same as Equation 2.1 from Röst and Sadeghimanesh (2021) for $n = 2$.

For a fixed choice of parameter values, a steady state or equilibrium of system (1) is a non-negative solution to the system of equations obtained by setting $\dot{N}_i = 0$ for $i = 1, 2$. Therefore, to study the number of steady states of our model, the following parametric system of polynomial equations needs to be studied:

$$\begin{aligned} N_1(1-N_1)(N_1-b) - \delta_{1,2}aN_1 + \delta_{2,1}aN_2 &= 0, \\ N_2(1-N_2)(N_2-b) + \delta_{1,2}aN_1 - \delta_{2,1}aN_2 &= 0, \end{aligned} \tag{2}$$

$$\text{variables: } N_1 \geq 0, \ \ N_2 \geq 0,$$
$$\text{parameters: } a \geq 0, \ \ 1 \geq b \geq 0.$$

Solving a parametric system of polynomial equations and giving an explicit formula for the solutions is not often an easy task or possible. Therefore in practice, especially in biology and ecology, one may need to get help from simulations (see Fernandez et al., 2012), or data from experiments (see Smith et al., 2014). However, simulations and experiments only provide information for a finitely many choices of the parameters and it is not always possible to conclude a general behavior or guarantee that other possible cases are not missed in the observations. On the other hand, there are algebraic tools developed to study the number of solutions of a parametric system of equations without solving the system and having a closed-form parametric solution formulae. We will use one of such tools that recently has attracted attention of many applied mathematicians and has been used in various applications successfully.

It is clear that in the absence of the spatial dispersal between the two patches, the system has 9 non-negative steady states for $b \in (0,1)$. In Sections 4 and 5 we concentrate on the two other connectivity cases shown in Figures 1b and 1c.

(a) (b) (c)

Figure 1: There are only three non-isomorphic digraphs on two nodes. (a) Two isolated nodes. (b) There are two directed edges between the two nodes. (c) There is one directed edge from one of the two nodes to the other one.

3 Tools from Computational Algebra

To better explain the algebraic concepts we step back in this section and pick up a smaller example. Consider a single population with strong Allee effect with the carrying capacity equal to 1 and the Allee threshold parameter equal to b. Denote the size of the population by x. Therefore the population is modelled by the following equation:

$$\dot{x} = x(1-x)(x-b). \tag{3}$$

To find the steady states we need to solve $\dot{x} = 0$ with the assumption $x \geq 0$. Though in this case it is straightforward to solve the equation explicitly, let us use another approach. Call the polynomial of Equation (3) by f, i.e., $f_b(x) = x(1-x)(x-b)$ with b as a parameter and x as a variable. While f can be seen as a function of both x and b, that is $f(x,b)$, we appreciate that considering b as a parameter means that we are looking at a family of functions in only x, that is $\{f_b(x) \mid b \in \mathbb{R}\}$ which contains $f_2(x) = x(1-x)(x-2)$ for example. For each choice of the parameter b, the solution set to $f_b(x) = 0$ is different. The equation $f_1(x) = 0$ has two real solutions, whereas $f_{0.5}(x) = 0$ has three real solutions. The set of parameter values where the number of solutions of a system of equations changes is called the *discriminant variety* of the system.

To find the discriminant variety we note that to lose a real root or to gain a new real root, we need to vary the value of the parameter, b, so that two real solutions become equal and then leave the real line and become complex conjugates or vice

versa. Hence, we need to cross the values of b for which the system has a solution of multiplicity higher than one. For any such value of b there exists a value of x such that (x, b) satisfies the system $f(x, b) = \frac{df}{dx}(x, b) = 0$. Therefore, the important values of b where the number of real solutions can change are the projections of the variety (solution set) of the system of equations $f(x, b) = \frac{df}{dx}(x, b) = 0$ into the b-axis. One can use elimination theory via Gröbner basis computation to compute this projection, (see Cox et al., 2015, Chapter 3). The corresponding algorithms are implemented in the Maple package called `PolynomialIdeals`. The command `EliminationIdeal` receives two inputs, the set of polynomials defining a system of equations, here $\{f(x, b), \frac{df}{dx}(x, b)\}$, and a set of variables corresponding to the coordinates that we want to project the solution set of the system into the linear subspace made by keeping only these coordinates, here $\{b\}$. The output of the algorithm is a set of polynomials only involving the variables corresponding to the coordinates that we want to keep such that its solution set is the smallest set containing the projection and can be written as a solution set of polynomial equations. In this example the Maple code is as the following:

```
f := x*(1-x)*(x-b);
PolynomialIdeals:-EliminationIdeal( PolynomialIdeals:-PolynomialIdeal( f, diff( f, x ) ), { b } );
```

For code details see (Röst and Sadeghimanesh, 2023).

Here the output consists of a single polynomial involving only b, that is $g(b) = b^2(b-1)^2$. It has only two roots $b = 0, 1$. Now the second step is to decompose the parameter space with respect to the discriminant variety. In our case this is easy. The parameter space, which is $R_{\geq 0}$ with respect to $\{0, 1\}$, can be decomposed to two open sets; $(0, 1)$ and $(1, \infty)$, and two closed sets $\{0\}$ and $\{1\}$. The sets in this decomposition are called cells. The important property of the cells of this decomposition with respect to the discriminant variety is that the number of real solutions of the system is invariant in each cell. In other words, for two choices of b from the same cell, the system has the same number of solutions. In this case the system has three solutions on the two open cells, and two solutions on the two closed cells.

In this case the computations are easy, but to do the decomposition in a structural and automatic way, an algorithm called cylindrical algebraic decomposition (CAD) has been introduced (Collins, 1975). We avoid explaining the CAD algorithm here and instead we refer the reader to Jirstrand (1995). Luckily an algorithm consisting of both steps of the method just introduced is already implemented in a Maple package called `RootFinding:-Parametric` (Gerhard et al., 2010). The reader also should note that when there are more restrictions on the solutions, such as non-negativity constraint, there are more components needed to be computed in the discriminant variety, we refer the interested reader to Lazard and Rouillier (2007); Moroz (2008) for a complete treatment of the discriminant variety. Note that CAD with respect to the discriminant variety has been used in other similar questions such as in chemical reaction network theory (Bradford et al., 2020; Lichtblau, 2021).

We investigate the parametric system in equation (2) using `RootFinding:-Parametric` library in Maple. In contrast with the case $n = 3$ from Röst and Sadeghimanesh (2021), the case $n = 2$ is not heavy for a simple computer to handle—computations performed on Windows 10, Intel(R) Core(TM) i7-2670QM CPU @ 2.20GHz 2.20 GHz, x64-based processor, 6.00GB (RAM). Thus without using any numerical algorithm one can get an exact description of the boundaries of different parameter regions where the system (2) has different number of non-negative solutions.

4 Bidirectional (Both Ways) Migration

Consider first the connectivity graph in Figure 1b. In this case $\delta_{1,2} = \delta_{2,1} = 1$. We first prove a generalized version of Lemma 2.1 from Röst and Sadeghimanesh (2021).

Lemma 4.1. *Let G be an arbitrary digraph with n nodes and $M = [\delta_{i,j}]$ be the adjacency matrix of G. Thus $\delta_{i,j} = 1$ if there is an edge from node i to node j, and 0 otherwise. Consider the following ODE system in n variables N_i, $i = 1, \dots, n$ and two parameters a and b.*

$$\dot{N}_i = N_i(1 - N_i)(N_i - b) - \left(\sum_{j=1, \delta_{i,j}=1}^{n} a \right) N_i + \sum_{j=1, \delta_{j,i}=1}^{n} a N_j, \qquad i = 1, \dots, n. \tag{4}$$

This ODE system corresponds to n identical patches with strong Allee effect and G as its connectivity graph associated with M. The number of steady states of (4) for the parameter choice $(a, b) \in \mathbb{R}^2_{>0}$ is equal to the number of steady states for the parameter point $\left(\frac{a}{b^2}, \frac{1}{b}\right)$.

Proof. Using the same change of variables as in the proof of Lemma 2.1 from Röst and Sadeghimanesh (2021), i.e., $y_i = \frac{N_i}{b}$,

$i = 1, \dots, n$, we have

$$\begin{aligned}
\dot{y}_i = \frac{\dot{N}_i}{b} &= \frac{1}{b}\left(N_i(1-N_i)(N_i-b) - \left(\sum_{j=1,\delta_{i,j}=1}^{n} a \right) N_i + \sum_{j=1,\delta_{j,i}=1}^{n} a N_j \right) \\
&= \frac{1}{b}\left(by_i(1-by_i)(by_i-b) - \left(\sum_{j=1,\delta_{i,j}=1}^{n} a \right) by_i + \sum_{j=1,\delta_{j,i}=1}^{n} a b y_j \right) \\
&= \frac{b^3}{b}\left(y_i(\frac{1}{b}-y_i)(y_i-1) - \left(\sum_{j=1,\delta_{i,j}=1}^{n} \frac{a}{b^2} \right) y_i + \sum_{j=1,\delta_{j,i}=1}^{n} \frac{a}{b^2} y_j \right) \\
&= b^2\left(y_i(1-y_i)(y_i-\frac{1}{b}) - \left(\sum_{j=1,\delta_{i,j}=1}^{n} \frac{a}{b^2} \right) y_i + \sum_{j=1,\delta_{j,i}=1}^{n} \frac{a}{b^2} y_j \right).
\end{aligned}$$

Hence for any solution $(x_1, \dots, x_n)$ of the system for the point (a, b), we have a solution $(\frac{x_i}{b}, \dots, \frac{x_n}{b})$ for the parameter point $(\frac{a}{b^2}, \frac{1}{b})$ and vice versa. This proves that the number of steady states (equilibria) of the system is the same for the two choices of the parameter points. □

When the connectivity graph G in Lemma 4.1 is a fully connected digraph, we get Lemma 2.1 from Röst and Sadeghimanesh (2021). On the other hand Lemma 2.2 of Röst and Sadeghimanesh (2021) states that the number of steady states of (4), when the connectivity graph is fully connected, for the choice of the dispersal rate and the Allee threshold $a \in \mathbb{R}_{>0}$ and $b \in (0,1)$, is equal to the number of steady states when the dispersal rate and the Allee threshold are set to a and $1-b$. Note that this lemma can not be generalized to an arbitrary connectivity graph. Therefore by these two lemmas, to study the number of steady states of (1) with fully connected connectivity graph, it is enough to restrict the parameter space to $0 \le b \le \frac{1}{2}$.

We used the Maple package `RootFinding:-Parametric` to decompose the parameter region $[0,\infty)\times[0,\frac{1}{2}]$ with respect to the number of steady states. The Maple worksheet containing the computations can be found in (Röst and Sadeghimanesh, 2023). The result is depicted in Figure 2, generated by the Maple code. There are three open regions where the system attains 9, 5 or 3 steady states on each of them. The equations defining the boundaries between these regions are also computed in the Maple code. The boundary between the regions with 9 and 5 steady states in Figure 2 is defined by the following equation.

$$g_1(a,b) = 4ab^4 - 36a^2b^2 - 8ab^3 - b^4 + 108a^3 + 36a^2b + 12ab^2 + 2b^3 - 36a^2 - 8ab - b^2 + 4a = 0.$$

The boundary between the regions with 5 and 3 steady states in Figure 2 where $0 < b < \frac{1}{2}$ is defined by the equation

$$g_2(a,b) = b^2 + 2a - b = 0.$$

Fix a value for b, say $b^\star$. A value $a = a^\star$ is said critical for a if the point $(a^\star, b^\star)$ is on one of the boundaries between different regions. For any $b \neq 0$, there exist two critical values for a. The sequences of the number of steady states for a fixed value of $b \neq 0$ when increasing a (considering only open regions) are always the same as listed below:

- 9, 5, 3.

When $a = 0$, there are 9 steady states, passing the first critical value of a, two pairs of steady states collide and disappear in saddle node bifurcation events. Passing the second critical value, two other steady states meet at the middle steady state and the two disappear in a pitchfork bifurcation event. This has been shown by Knipl and Röst (2016, Figure 1a) where $b = 0.3$. Indeed in this case, the two connected populations has a simple behavior as was initially guessed.

5 Unidirectional (One-Way) Migration

Consider next the connectivity graph in Figure 1c. In this case $\delta_{1,2} = 1$, but $\delta_{2,1} = 0$. By Lemma 4.1, the parameter region necessary to study is $0 \le b \le 1$. The Maple package `RootFinding:-Parametric` is used to decompose the parameter region $[0,\infty) \times [0,1]$ with respect to the number of steady states. The result is depicted in Figure 3. There are four regions where the system has 9, 7, 5 and 3 steady states. These four regions are separated by two curves defined by the following two polynomials.

$$\begin{aligned}
g_3(a,b) = {} & 16a^3b^6 + 16a^2b^7 - 4ab^8 + 108a^4b^4 + 60a^3b^5 - 75a^2b^6 + 10ab^7 + b^8 - 54a^4b^3 - 12a^3b^4 + 42a^2b^5 \\
& + 4ab^6 - 4b^7 + 729a^6 + 1458a^5b + 405a^4b^2 - 328a^3b^3 + 50a^2b^4 - 20ab^5 + 6b^6 - 54a^4b - 12a^3b^2 \\
& + 42a^2b^3 + 4ab^4 - 4b^5 + 108a^4 + 60a^3b - 75a^2b^2 + 10ab^3 + b^4 + 16a^3 + 16a^2b - 4ab^2, \\
g_4(a,b) = {} & -b^2 + 4a + 2b - 1.
\end{aligned}$$

The region with 9 steady states is between the b-axis, $g_3(a,b) = 0$, and $g_4(a,b) = 0$; the region with 7 steady states is surrounded by $g_3(a,b) = 0$; the region with 5 steady states is between the a-axis, $g_3(a,b) = 0$, and $g_4(a,b) = 0$; and finally the region with 3 steady states is on the right side of $g_4(a,b) = 0$.

In contrast with the previous case, the number of critical values for a are not always the same for fixed values of b. We refer to the values of b where the number of critical values for a changes as critical values for b. We found that (details are in Maple file) the critical values for b are 0, 1, β_1, and β_2, where $\beta_2 = 1/2$, and β_1 is an algebraic number, specifically the smallest positive real root of $59b^4 - 16b^3 - 214b^2 - 16b + 59$. With seven digits accuracy, $\beta_1 \simeq 0.4961661$. In fact β_1 and β_2 are the b-coordinates of two points on the curve $g_3(a,b) = 0$. The curve has a horizontal tangent line at the first point, and the second point is where this curve intersect the other curve, $g_4(a,b) = 0$. See Figure 3b. For a fixed value of b, let $\alpha_i(b)$, $i = 1, 2, 3$ be the values of a for which (a,b) is on a boundary between two regions, ordered from the smallest value to the largest. We drop the emphasis on b and simply write α_i.

The sequences of the number of steady states for a fixed value of b when increasing a (considering only open regions) are listed below:

- 9, 7, 5, 3.
- 9, 7, 9, 3.
- 9, 3.

The region where the increment in the number of steady states happens is enlarged at Figure 3b. See also Table 1 for the detailed description of the parameter regions with different number of steady states.

Figure 2a in (Knipl and Röst, 2016) has shown the sequence of steady states for $b = 0.3$ where the temporary increment in the number of steady states does not happen.

Figure 4 shows the five possible sequences for $b \neq 0, 1$ (including the cases $b = \beta_1$ and $b = 0.5$) together with the stability of the steady states. Figure 5 is a schematic figure simplifying the behavior of the system for these 5 cases. All bifurcation events here are saddle-node except at two points. At $b = 0.5$, by increasing a to cross its first critical value, a transcritical bifurcation event happens where two steady states meet and then continue their paths. At $b = \beta_1$, by increasing a to cross its second critical value, two steady states that already had met and left the real plane return at exactly the location where another pair of steady states are meeting to leave the real plane. Therefore at this moment, there are four steady states at a single point.

6 Discussion

Knipl and Röst (2016) stated that for small enough dispersal rate, the n patches model has 3^n steady states and generally the situation simplifies with increased migration, eventually leading to only 3 steady states resembling a simple one larger patch consisting of all populations mixed together. It was expected to see a monotone decrease in the number of steady states by increasing the dispersal rate until Vortkamp et al. (2020, for the discrete version of this model) and Röst and Sadeghimanesh (2021, for $n = 3$) showed that the behaviour can be more complex than it might look at an initial thought. The authors of this paper have completely classified all possible bifurcations for the case $n = 3$ in (Röst and Sadeghimanesh, 2021) and have shown that a temporary increment in the number of steady states can occur for specific choices of the Allee threshold, provided that all patches are connected by both ways migration. Here we demonstrated that we can see an increment in the number of steady states even for the case $n = 2$, if we allow only one-way migration. Using algebraic methods and well established algorithms, we confirm that, for bidirectional migration, there is only one bifurcation sequence resulting in 9, 5, 3 steady states, respectively, as the migration rate increases. However, if the migration is only one-way, there is a variety of bifurcation sequences that we fully classify in Table 1, Figure 4, and Figure 5. Our results illustrate that the bifurcations generated by spatial dispersal of species in the presence of Allee effect are much more involved than one might think, even in simple looking situations such as two patches.

These results have practical implications in spatial ecology. Due to environmental changes, migration can either intensify or diminish, hence it is important to describe how the population dynamics is effected by such changes, which can be understood by the bifurcation sequences we characterized. A relevant observation made by Keitt et al. (2001) from patch models that the spatial range of a species habitat is more stable (less prone to expansion and shrinking) when Allee effect is present. Studying three different ecosystem models on patches arranged on a one-dimensional lattice, van Nes and Scheffer (2005) concluded that if the dispersion between patches is small, then the system responds to global changes in a gradual manner, rather than a catastrophic way. According to them, the idea that dispersal can make heterogeneous systems behave like single homogeneously mixed systems is intuitively straightforward. However, it is not as straightforward when Allee effect also occurs. For small dispersal the system is similar to a disconnected set of patches which can be investigated individually (see the perturbation approach of Knipl and Röst, 2016), and Röst and Sadeghimanesh (2021) showed that, by increasing the dispersal rate between three patches, the steady state structure indeed becoming identical to a homogeneous well mixed system. But Röst and Sadeghimanesh (2021) also showed that in between, complicated bifurcations can occur for moderate levels of dispersal. As we illustrated in this paper, the situation can be complicated even for two patches, if the migration is unidirectional. To determine optimal levels of dispersal under Alleee

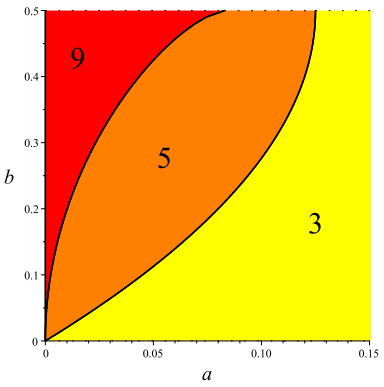

Figure 2: The parameter region $0 \le b \le \frac{1}{2}, a \ge 0$ of the 2 patches model (1) with the connectivity graph as shown in Figure 1b is partitioned to sub-regions with invariant number of steady states. The number of steady states is written on each open region.

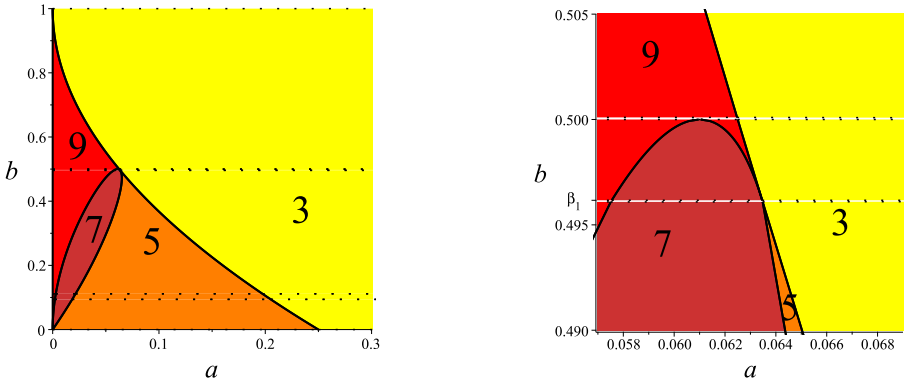

(a) $0 \le b \le 1$ (b) $\beta_1 < b < 0.5$

Figure 3: (a) The parameter region $0 \le b \le 1, a \ge 0$ of the two patches model (1) with the connectivity graph as shown in Firgure 1c is partitioned to sub-regions with invariant number of steady states. (b) When $\beta_1 < b < 0.5$ the number of steady state temporary increases when increasing a, this region is the tiny red colored part between the brown and yellow regions.

Table 1: The number of non-negative steady states of the the two patches model (1) with the connectivity graph as shown in Firgure 1c for the parameters $a \ge 0, 0 \le b \le 1$. The first column shows the interval of b. Each row for the intervals of b has two sub-rows, the first sub-row shows the interval of a and the second sub-row states the number of steady states.

b	a number of steady states						
$\{0\}$	$\{0\}$	$(0,\infty)$					
	4	2					
$(0,\beta_1)$	$[0,\alpha_1)$	$\{\alpha_1\}$	(α_1,α_2)	$\{\alpha_2\}$	(α_2,α_3)	$\{\alpha_3\}$	(α_3,∞)
	9	8	7	6	5	4	3
$\{\beta_1\}$	$[0,\alpha_1)$	$\{\alpha_1\}$	(α_1,α_2)		$\{\alpha_2=\alpha_3\}$		(α_3,∞)
	9	8	7		5		3
(β_1,β_2)	$[0,\alpha_1)$	$\{\alpha_1\}$	(α_1,α_2)	$\{\alpha_2\}$	(α_2,α_3)	$\{\alpha_3\}$	(α_3,∞)
	9	8	7	8	9	6	3
$\{\beta_2\}$	$[0,\alpha_1)$		$\{\alpha_1=\alpha_2\}$		(α_2,α_3)	$\{\alpha_3\}$	(α_3,∞)
	9		8		9	6	3
$(\beta_2,1)$	$[0,\alpha_1)$		$\{\alpha_1=\alpha_2=\alpha_3\}$				(α_3,∞)
	9		6				3
$\{1\}$	$\{0\}$	$(0,\infty)$					
	4	2					

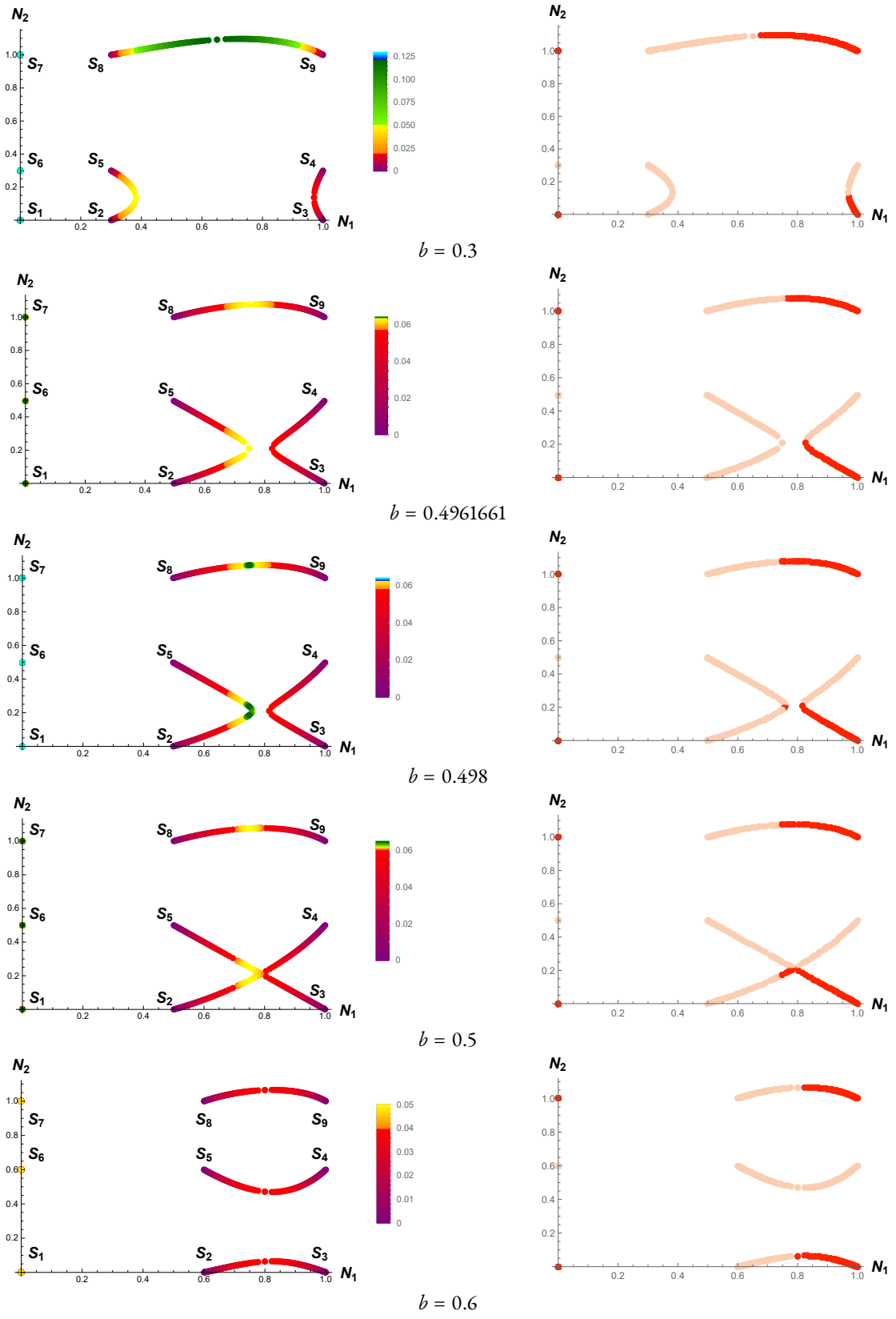

Figure 4: Sequences of the steady states for fixed values of b, but varying values of a. In the left side the steady state points are colored with respect to the value of a that can be read from the color bar next to the plots. In the right side the steady states are colored with respect to their stability. Stable steady states are colored by red, whereas the unstable ones are colored by pink.

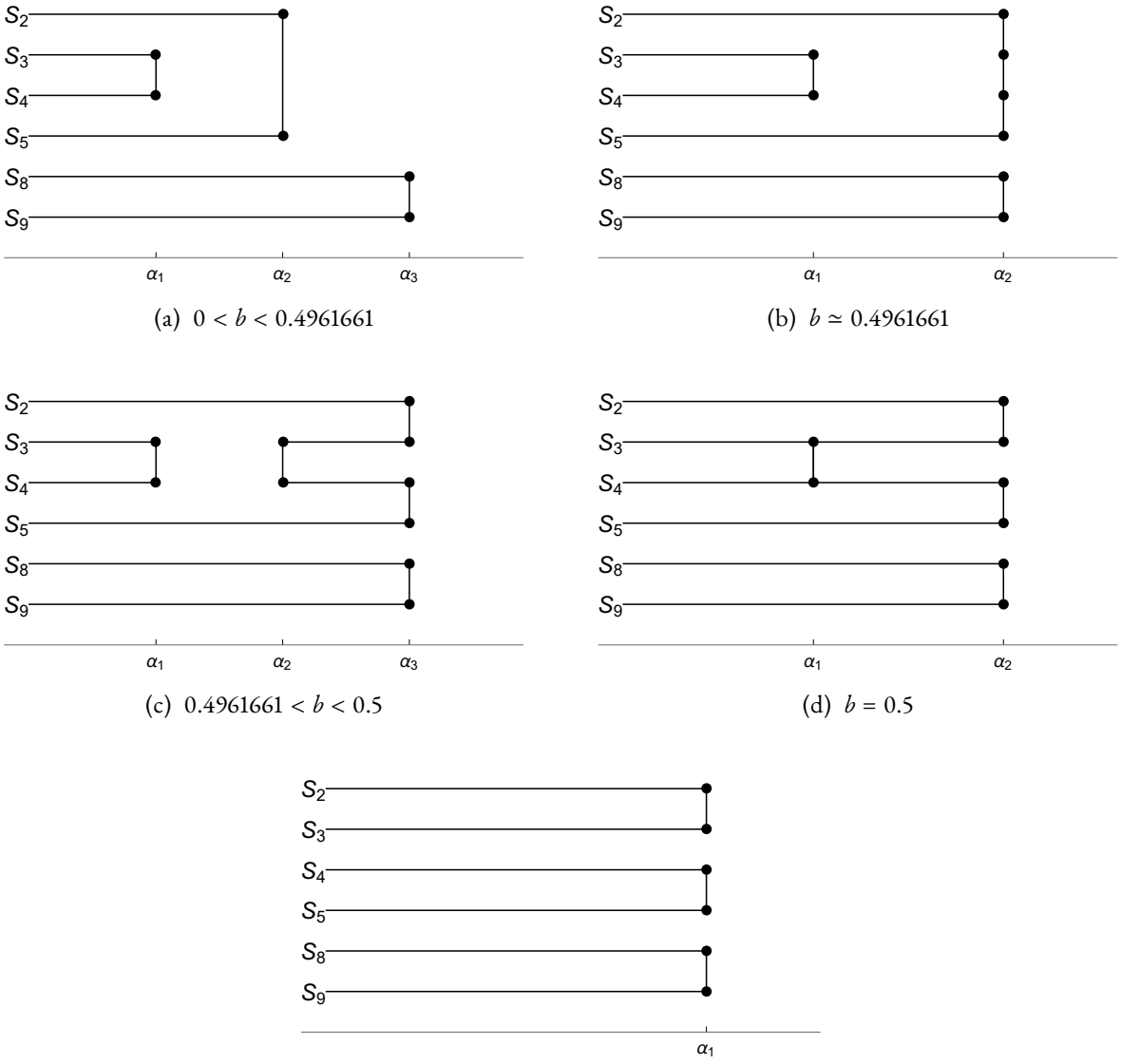

(a) $0 < b < 0.4961661$

(b) $b \simeq 0.4961661$

(c) $0.4961661 < b < 0.5$

(d) $b = 0.5$

(e) $0.5 < b < 1$

Figure 5: Schematic plots showing when and which of the initial 9 steady states of the 2 patches model (1) with the connectivity graph Figure 1c collide and disappear. The initial nine steady states for $a = 0$ are shown at Figure 4 which are $S_1 = (0,0)$, $S_2 = (b,0)$, $S_3 = (1,0)$, $S_4 = (1,b)$, $S_5 = (b,b)$, $S_6 = (0,b)$, $S_7 = (0,1)$, $S_8 = (b,1)$ and $S_6 = (1,1)$. In contrast with the initial guess that by increasing a, the steady states only meet and disappear, as one can see in (c) two steady states that previously have met and went out of the real plane, can meet again and return from the non-real complex plane back to the real plane. The horizontal line shows the values of a which is 0 at the left and increases as we move to the right. All bifurcation events are of the saddle-node type, except at $a = \alpha_2$ in part (b) and at $a = \alpha_1$ in part (d). In the first case, the two steady states S_3 and S_4 are coming back at the same location where S_2 and S_5 are meeting and then all four of them leave the real plane. At the second case, a transcritical bifurcation occurs. S_3 and S_4 meet and then continue their paths.

effect in a stochastic metapopulation model, that maximizes the survival probability of the species, an agent based model was implemented by Pires and Duarte Queirós (2019), with an empirical underpinning.

For more specific examples, colony collapse disorder in honeybees were associated with varying levels of mite migration in a two patch model by Messan et al. (2017), and the vulnerability of hives under Allee effect was pointed out by Kribs-Zaleta and Mitchell (2014). Yet, the combination of these factors have not been analyzed yet.

Finally, we discuss the connections of our results to a recent study by Greiner et al. (2022) on coral reef conservation, where they studied the effect of dispersal and Allee effect, and hereby we quote some relevant conclusions of that work. Their findings indicate that changing dispersal levels (which can be due to climate change, or reef degradation) between reefs changes the possible stable states. Here, we described all possible steady states by changing the dispersal level as bifurcation parameter, and detected the critical levels where new steady states appear. Moreover, the combination of dispersal and local bistability (emerging from Allee effect) in a system of two interconnected coral reefs was predicted to lead to new dynamics and a new type of stable state, where both reefs have some coral cover and some macroalgae cover. Their model also predicted that these states are stable at even higher coral dispersal levels, when the macroalgal dispersal level is set to be lower than the coral dispersal level. By incorporating spatial dispersal into the ecological model, an explanation is offered to past empirical findings that puzzled researchers. The authors call for follow-up works which should focus on temporally changing, as well as asymmetric dispersal levels (here we studied a special asymmetric case, the unidirectional dispersal), and their impact on the dynamics in systems of multiple reefs in a more complex network structure. Furthermore, they conclude that careful consideration of coral reef dispersal levels in the design of coral reef fisheries and conservation management plans may be essential for conserving coral reef ecosystems and thus sustaining the livelihoods and food security of millions of people around the world.

Overall, future works on the analysis of more complicated patch models with migration and Allee effect is motivated by mathematical interests as well as ecological relevance.

Data access statement. The code files of the computations and the plots of this paper are openly available from this URL: https://doi.org/10.5281/zenodo.7602284.

Acknowledgements. Gergely Röst was supported by Hungarian grants NKFIH FK 124016, RRF-2.3.1-21-2022-00006, and TKP2021-NVA-09. AmirHosein Sadeghimanesh was funded by NKFIH KKP 129877.

References

Bradford, R., J. H. Davenport, M. England, H. Errami, V. Gerdt, D. Grigoriev, C. Hoyt, M. Košta, O. Radulescu, T. Sturm, and A. Weber (2020). Identifying the parametric occurrence of multiple steady states for some biological networks. *Journal of Symbolic Computation 98*, 84–119. Special Issue on Symbolic and Algebraic Computation: ISSAC 2017. 45

Collins, G. E. (1975). Quantifier elimination for real closed fields by cylindrical algebraic decompostion. In *Automata Theory and Formal Languages*, Berlin, Heidelberg, pp. 134–183. Springer Berlin Heidelberg. 45

Courchamp, F., L. Berec, and J. Gascoigne (2008). *Allee effects in ecology and conservation*. Oxford University Press. 43

Cox, D. A., J. Little, and D. O'Shea (2015). *Ideals, Varieties, and Algorithms: An Introduction to Computational Algebraic Geometry and Commutative Algebra*. Springer-Verlag. 45

Fernandez, A. A., T. Hance, and J. L. Deneubourg (2012). Interplay between allee effects and collective movement in metapopulations. *Oikos 121*(6), 813–822. 44

Gerhard, J., D. J. Jeffrey, and G. Moroz (2010). A package for solving parametric polynomial systems. *ACM Communications in Computer Algebra - Sigsam 43*(3/4), 61–72. 45

Greiner, A., E. S Darling, M.-J. Fortin, and M. Krkošek (2022). The combined effects of dispersal and herbivores on stable states in coral reefs. *Theoretical Ecology 15*(4), 321–335. 51

Gyllenberg, M., J. Hemminki, and T. Tammaru (1999). Allee effects can both conserve and create spatial heterogeneity in population densities. *Theoretical population biology 56*(3), 231–242. 43

Jirstrand, M. (1995). Cylindrical algebraic decomposition - an introduction. Retrieved from Linköping University website: http://urn.kb.se/resolve?urn=urn:nbn:se:liu:diva-55291. 45

Keitt, T. H., M. A. Lewis, and R. D. Holt (2001). Allee effects, invasion pinning, and species' borders. *The American Naturalist 157*(2), 203–216. 43, 47

Knipl, D. and G. Röst (2014). Large number of endemic equilibria for disease transmission models in patchy environment. *Mathematical Biosciences 258*, 201–222. 43

Knipl, D. and G. Röst (2016). Spatially heterogeneous populations with mixed negative and positive local density dependence. *Theoretical Population Biology 109*, 6–15. 43, 44, 46, 47

Kribs-Zaleta, C. M. and C. Mitchell (2014). Modeling colony collapse disorder in honeybees as a contagion. *Mathematical Biosciences & Engineering 11*(6), 1275. 51

Lazard, D. and F. Rouillier (2007). Solving parametric polynomial systems. *Journal of Symbolic Computation 42*(6), 636–667. 45

Lichtblau, D. (2021). Symbolic analysis of multiple steady states in a mapk chemical reaction network. *Journal of Symbolic Computation 105*, 118–144. 45

Messan, K., G. DeGrandi-Hoffman, C. Castillo-Chavez, and Y. Kang (2017). Migration effects on population dynamics of the honeybee-mite interactions. *Mathematical modelling of natural phenomena 12*(2), 84–115. 51

Moroz, G. (2008). *Sur la décomposition réelle et algébrique des systémes dépendant de paramétres*. Ph. D. thesis, Université Pierre et Marie Curie - Paris VI. https://tel.archives-ouvertes.fr/tel-00812436/file/these_moroz.pdf. 45

Okubo, A. and S. A. Levin (2001). *Diffusion and ecological problems: modern perspectives*, Volume 14. Springer. 43

Pires, M. A. and S. M. Duarte Queirós (2019). Optimal dispersal in ecological dynamics with allee effect in metapopulations. *PloS one 14*(6), e0218087. 51

Röst, G. and A. Sadeghimanesh (2021). Exotic bifurcations in three connected populations with allee effect. *International Journal of Bifurcation and Chaos 31*(13), 2150202. 44, 45, 46, 47

Röst, G. and A. Sadeghimanesh (2023). The computation codes for the paper "Unidirectional migration of populations with allee effect". DOI: 10.5281/zenodo.7602284. 43, 45, 46

Smith, R., C. Tan, J. K. Srimani, A. Pai, K. A. Riccione, H. Song, and L. You (2014). Programmed Allee effect in bacteria causes a tradeoff between population spread and survival. *Proceedings of the National Academy of Sciences 111*(5), 1969–1974. 44

van Nes, E. H. and M. Scheffer (2005). Implications of spatial heterogeneity for catastrophic regime shifts in ecosystems. *Ecology 86*(7), 1797–1807. 47

Vortkamp, I., S. J. Schreiber, A. Hastings, and F. M. Hilker (2020). Multiple attractors and long transients in spatially structured populations with an Allee effect. *Bulletin of Mathematical Biology 82*(6), 1522–9602. 43, 47